

Received February 27, 2020, accepted March 14, 2020, date of publication March 20, 2020, date of current version April 6, 2020.

Digital Object Identifier 10.1109/ACCESS.2020.2982184

Automatic Phase Picking From Microseismic Recordings Using Feature Extraction and Neural Network

TIANQI JIANG¹ AND JING ZHENG²

¹College of Geoscience and Surveying Engineering, China University of Mining and Technology (Beijing), Beijing 100083, China

²State Key Laboratory of Coal Resources and Safe Mining, China University of Mining and Technology at Beijing, Beijing 100083, China

Corresponding author: Tianqi Jiang (jiang_tianqi0623@163.com)

This work was supported in part by the China National Key Research and Development Program under Grant 2018YFB0605503, in part by the National Natural Science Foundation of China under Grant 41504041, in part by the 111 Project under Grant B18052, and in part by the Yue Qi Young Scholar Project, China University of Mining and Technology, Beijing.

ABSTRACT High-accuracy microseismic phase picking is fundamental to microseismic signal processing. Phase picking methods based on deep learning show great potential dealing with low signal to noise ratio (SNR) data but need enormous training data. However, it's not easy to obtain a big size of field datasets and label them manually to train the neural network. In this paper, a novel method is proposed by applying feature extraction (Gammatone Feature) and neural networks to pick phases automatically. The feature extraction scheme aims to train the neural network using a relatively small size of training datasets. To test the performances of the proposed method, synthetic datasets were obtained by numerical simulation and used to train the neural network. Both synthetic datasets and field datasets were used to test the neural network for picking P- and S-phases of microseismic events. The results of phase picking illustrate that: (1) feature extraction scheme in the training stage can help reduce the size of training datasets; (2) The neural network can be trained well just by synthetic data and phase picking results are accurate and satisfying when the method was tested by both synthetic and field datasets.

INDEX TERMS Feature extraction, Gammatone feature, neural networks, phase picking.

I. INTRODUCTION

Automatic phase picking of microseismic is important for many geophysical prospecting methods, such as seismic/acoustic emission (AE)/microseismic systems [1]. Many researchers have studied this area and proposed methods for automatic phase picking of microseismic signals. Some methods are based on energy ratio between signal and noise, these classical or improved approaches calculate Short Time Average over Long Time Average (STA/LTA) to pick arrival time [2], [3]. The energy ratio-based methods can't perform well when dealing with low SNR microseismic data so many researches applied noise suppression schemes to enhance the signals. Time-frequency transform is an effective way to suppress noise such as Intrinsic Time-Scale Decomposition based time-frequency energy denoising, Hilbert–Huang transform (HHT), apex-shifted parabolic Radon transform (ASPR), adaptive directional vector median filters, wavelet transform and so on [4]–[10].

The associate editor coordinating the review of this manuscript and approving it for publication was Utku Kose.

Automatic phase pickers are essential because microseismic monitoring is a real-time process [11]. And also some researches focus on improving performances of automatic pickers by introducing neural networks [12]. The neural networks have already been used to pick the arrival times automatically for downhole microseismic surveys [13]. CNN, DNN and RNN network can achieve to pick P and S phases with three-component seismograms [14]–[17]. Some previous work focused on inputting derived attributes from seismic data into a hybrid artificial neural network for phase picking [18], [19]. These works prove that neural networks have advantages in phase picking. But Neural networks need large size training datasets with labels and it's time-consuming to label the datasets manually.

Although deep learning neural networks can pick phases of microseismic events automatically but good performances of neural networks need a big amount of labeling datasets. In this paper, we proposed a method to pick phases with the Gammatone feature (GF) stream and the neural network. A dictionary, also as a redundant system, constructed by GF can represent microseismic datasets sparsely and these

sparingly represented datasets can help reduce the size of neural networks, which means that we can train the network with less parameter, smaller size of training data and less computing time. In the network training stage, relatively small size synthetic datasets were used for updating weights of each neural unit. In the testing stage, we tested the network model with both synthetic and field datasets. The results illustrated that the model can pick phases of microseismic events from recordings with different SNR. The proposed scheme has two advantages: first, the model can be trained by using the relatively small size of synthetic datasets and then applied field datasets to the network for microseismic phase picking, a smaller size training data means less amount of calculation and labeling work; second, with different labeling strategies the model can realize different phase picking effects according to different demands. Two examples are shown in the paper, the first one is to pick events caused by human activities (footsteps); the second one is to recognize different microseismic phases (P-phase and S-phase).

II. METHOD

The general block scheme of the proposed method is shown in Fig. 1.

There are two main steps to train the neural network for phase picking. The first step is feature extraction by which we can obtain the Gammatone feature (GF) of datasets. These extracted features are regarded as the input data of the neural network. The second step is to train the network using GF obtained in the first step. The outputs of the neural network are the classification results (microseismic phase or noise).

The dominant frequency of microseismic events is far less than the sampling rate. Besides, signals of interests (microseismic events) are distributed in the low-frequency domain while noise is distributed over the full frequency band. To extract features of signals of interests, the filter bank should be of high resolution in the low-frequency domain and low resolution in the high-frequency domain. The characteristic of the filter bank mentioned above can help extract features of interests in noisy microseismic data. Considering the similarity of audio and microseismic recordings, we chose the Gammatone features as a robustness feature of microseismic recordings. GF is derived by cochleagrams of microseismic recordings and obtained by an auditory filter bank consisting of the Gammatone filters. Gammatone filter (GTF) is a linear filter that is an impulse response of the product of a gamma distribution and sinusoidal tone. It is a widely used model of auditory filters in the auditory system [20].

The Gammatone impulse response is given by

$$g(f, t) = at^{\alpha-1}e^{-2\pi bt} \cos(2\pi ft + \phi) \tag{1}$$

where a is gain of the filter, t is time, α is the order of the filter, b is decay factor, ϕ is phase and f is central frequency.

The detailed implementation of GF can be achieved as reference [21]. The formula of center frequency information

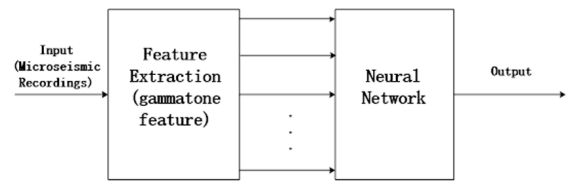


FIGURE 1. The proposed scheme.

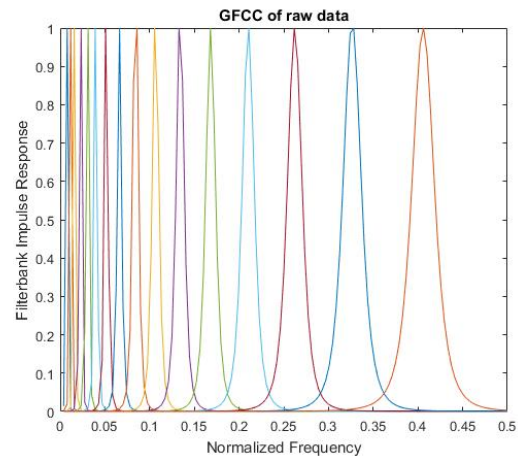


FIGURE 2. Filter bank impulse response, there are 16 colored curves representing frequency responses of each filter in the filter bank.

can be described as:

$$f(n) = -QB_0 + (f_H + QB_0) \exp\left(-\frac{n}{N} \ln\left(\frac{f_H + QB_0}{f_L - QB_0}\right)\right) \tag{2}$$

According to reference [22], $Q = 9.26449$, $B_0 = 24.7$, f_H and f_L are the maximum and minimum frequency of the filter bank. n means the n -th filter in the Gammatone filter bank. N is the number of filters in the Gammatone filter bank.

The impulse responses of 16 Gammatone filters are shown in Fig.2. There are 16 colored curves representing frequency responses of each filter in the filter bank. Here we want to talk further about GF, and filter bank impulse curves in Fig.2 show that the majority of filters are in the low-frequency domain and these filters are narrow-banded while the rest of filters are broad-banded and in high-frequency domain. The filter-bank constructed like this leads to higher resolutions of GF in the low-frequency domain. The proposed method benefits from doing this because (1) dominant frequencies of microseismic datasets are not very high so the extracted features of microseismic events should be represented by filters with high resolution in the low-frequency domain; (2) broad-band filter on higher frequencies means that the most of energies of noise would project on the components of GF in the higher frequency domain, this can help us extract target information (low-frequency events) from GF.

To obtain GF of microseismic recordings, inputs (microseismic recordings) are divided into data frames and the

outputs of the Gammatone filters are:

$$G_m(i) = GF(i, m) = [|g|(i, m)]^{1/3} \times (i = 0, 1, \dots, N - 1; m = 0, 1, \dots, M - 1) \quad (3)$$

$G_m(i)$ is a $N \times N$ matrix of Gammatone features (GF), $|g|(i, m)$ is the frequency spectrum obtained by of i -th filter with m -th data frame. N is the number of filters and M is the number of frames of recordings. For a certain data frame, a GF is a column of matrix $G_m(i)$.

As for $|g|(i, m)$, we frame the recordings and note the data frame as $x(l)$ and pre-emphasis the frame data as

$$y(l) = x(l) - 0.97 \times x(l - 1) \quad (l = 2, \dots, L) \quad (4)$$

Then a Hamming-window $w(l)$ is applied to the $y(l)$, the windowed data is

$$s(l) = y(l) \times w(l) \quad (5)$$

The windowed frame data is transformed from time domain to the frequency domain and noted as:

$$X(k) = FFT\{s(l)\} \quad (k = 1, \dots, K) \quad (6)$$

The data matrix $X_{K \times M}$ is constructed by each $X(k)$. according to references [23] and [24], a matrix of weights can be generated combining Fast Fourier Transform (FFT) matrix into gammatone matrix $W_{N \times K}$. And finally $|g|(i, m)$ in (3) is

$$|g|(i, m) = W_{N \times K} \times X_{K \times M} \quad (7)$$

The gammatone features are obtained using (3) and (7). $|g|(i, m)$ is a $N \times M$ matrix which means that in a certain m -th data frame, the length of extracted features of the data is N . In this study, we don't use the GF directly but post-process GF by applying post-processing technique to measure the GF flatness through a recursive scheme. The post-processing technique is described as follow:

$$\begin{aligned} L(i, m) &= GM(i, m + ns)/AM(i, m + ns) \\ GM(i, m + ns) &= Kg[GF^2(i, m + ns)] \\ &\quad + (1 - Kg)GM(i, m + ns - 1) \\ AM(i, m + ns) &= Ka[GF^2(i, m + ns)] \\ &\quad + (1 - Ka)AM(i, m + ns - 1) \end{aligned} \quad (8)$$

ns was regarded as the half length of the wavelets in recordings, Kg and Ka are set to be $1/ns$ and $Kg/4$ respectively. Now we got the post-process the Gammatone features and treated them as input data to the input layer of the neural network.

The extracted feature of microseismic recordings is ready for training the network and the neural network should go through two phases (training phase and testing phase) for automatic phase picking. In the training phase, the training process is to model the neural Networks mathematically. The weights among each layer are found iteratively. In the testing phase, the testing process is to recognize the phases of microseismic events. The neural networks have a fully connected hierarchical structure where the first layer is the

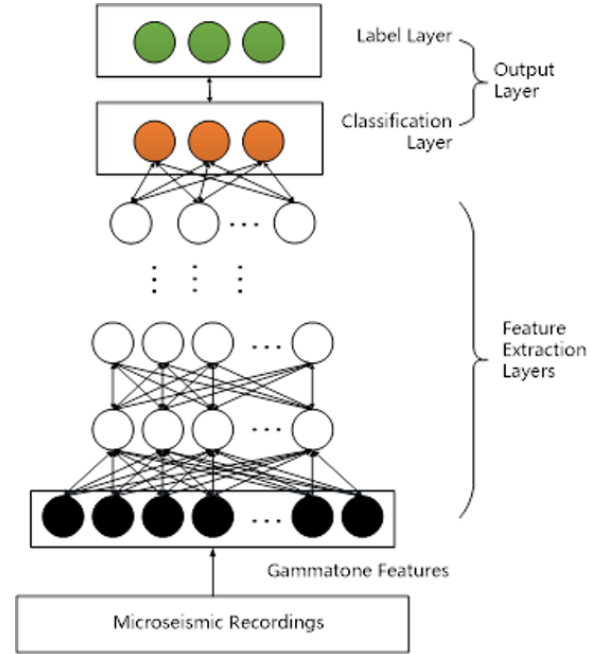


FIGURE 3. The proposed network model.

input layer; the highest layer is the output layer as shown in Fig. 3. The output layer of the network is a classification result. In our case, we used multiple restricted Boltzmann machines (RBMs) to stack the network to realize an unsupervised training process and after that a fine-tuning process with back-propagation algorithm (BP) is added to the network to achieve a supervised training process [25]. To realize fine-tuning process, a layer with labels is added to the output layer. The label consists of the manually picked phases (labels) of microseismic events. Parameters of the network model are initialized by RBM, the classification of the output layer is done by multiple classification logistic regression layers, the label layer is used to evaluate the error between the predictive output and the artificial picking phases. The optimization is achieved by stochastic gradient descent (SGD) strategy.

What makes the neural network special in this paper is that the microseismic datasets are not inputted into the network directly but using GF as the input data for the first layer. The aim of feature extraction scheme (GF) is to help reduce the size of training datasets and labeling work.

In microseismic monitoring tasks, the events are expressed as time series. There are different label strategies for different demands. In this study, we had two strategies for different tasks. One is to label the recordings as “None-zero” during the whole period of events and “Zero” for other time duration, we can note “1” for microseismic events and “0” for noise. To pick microseismic events in continuous recordings, we will rely on GF streams and train the network with event/non-event labeled datasets. We will apply this labeling strategy to one-component microseismic datasets to pick events caused by footsteps.

The other strategy is to label the first half period of the microseismic event as “None-zero” to get more sharp pickers for picking P and S phases. We can note “0” for noise, “1” for P-events and “2” for S-events. The classification layer has 3 classifying results namely noise, P-phase and S-phase. We label them as (1, 0, 0), (0, 1, 0), (0, 0, 1). If more phases are needed to be picked, we can just add neural units in the classification layer and label recordings with the same strategies. Meanwhile, we post-processed GF features by applying post-processing technique to measure the GF flatness through a recursive scheme according to (7) and (8). Then GF is used for training the neural network to pick different phases automatically. In the testing stage, the proposed method was applied to both synthetic datasets and field datasets, results of phase picking will be discussed in the next section.

III. EXPERIMENTAL ANALYSES

We designed two experiments for the different demands and analyzed performances of the proposed method. The network was firstly trained by synthetic datasets obtained by numerical simulations and then white noise of different intensities was added to the raw data. The performances of the proposed method were measured by investigating the accuracy rate of the testing stage. We used 1-C datasets for the first experiment and 3-C datasets for the second one. The 1-C Field datasets were obtained by 1-C vibration sensors, the microseismic events resulted from footsteps. The 3-C Field datasets were obtained by three-component geophones installed on the surface and the microseismic events were caused by hydraulic fracturing.

In this paper, we want to build an automatic phase picking model by using synthetic datasets and apply the model to field datasets to pick phases. We built two models including different label strategies according to different monitoring tasks. Firstly, we built the model only to pick microseismic events but not to identify the type of phases (P- or S- phase). Therefore, we labeled the datasets as “1” during the entire event period and “0” for the noise. Secondly, we built the model to identify the P- and S- phases of microseismic events. Therefore, we used 3-component datasets and labeled them as “1” only for the first half period of P- event, “2” for the first half period of S- event and “0” for noise.

Furthermore, we also used the same dataset to train the network without feature extraction. Comparing the results obtained by networks with/without feature extraction, they illustrated that GF can help reduce the demand for the size of training data and the proposed method for phase picking is accurate. The analyses are as followed.

A. ONE-COMPONENT DATASET MODEL TO PICK EVENTS

we used the synthetic datasets obtained by acoustic wave function to simulate one component recordings. The datasets are divided into two parts: about 70% of all are training datasets and the rest are testing datasets. The average SNR is 10dB. In the experiment, a four-layer neural network with two hidden layers is designed. The activation function of

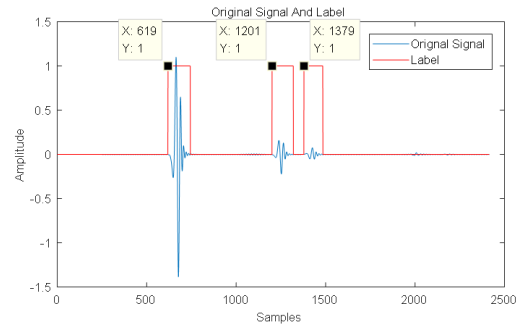


FIGURE 4. Manual labels of 1-Component datasets.

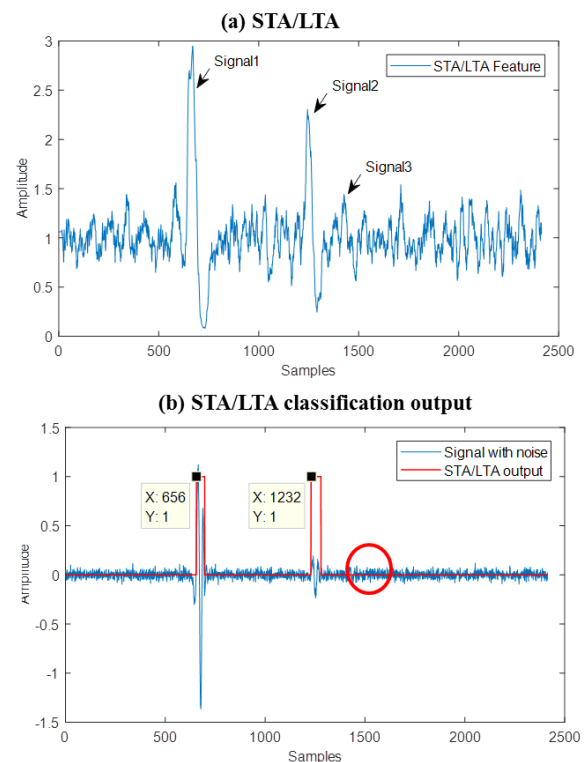


FIGURE 5. STA/LTA feature and classification output.

each layer is the sigmoid function. The training datasets were transformed into a GF matrix by a 64-Gammatone filter bank so the length of a GF is 64. Considering that the dominant frequency of wavelet in recordings is always low compared to the sampling frequency, we only maintained the results of first thirty Gammatone filters so the length of GF turns to 30. The number of neural units in each layer is 30, 20, 10 and 2 respectively. The length of the two hidden layers is 20 and 10. The length of the output layer is 2 because there are 2 classifications (event and noise).

We selected a trace of synthetic data to evaluate the performance of the proposed method. The raw data with manual labels are shown in Fig.4. There are three events in the time series. White noise of different intensities was added to the raw data and the noisy data is shown in Fig.5(b).

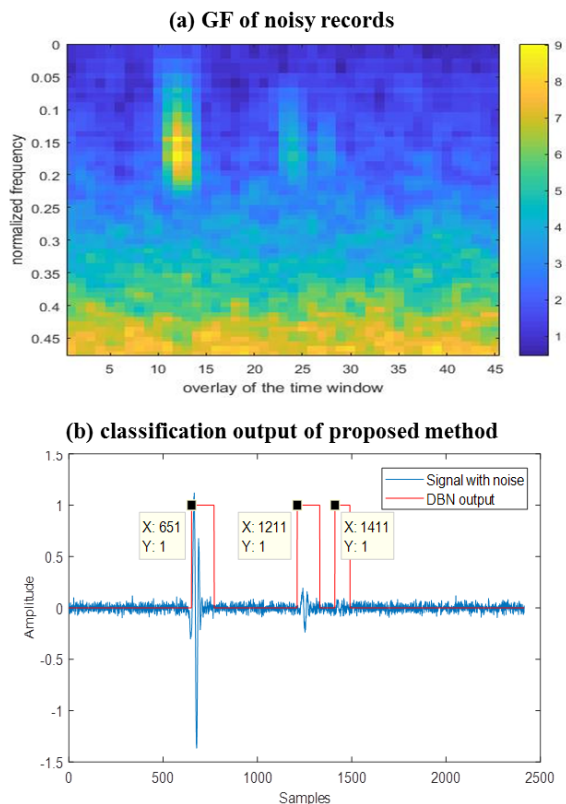


FIGURE 6. Synthetic datasets and event picking outputs.

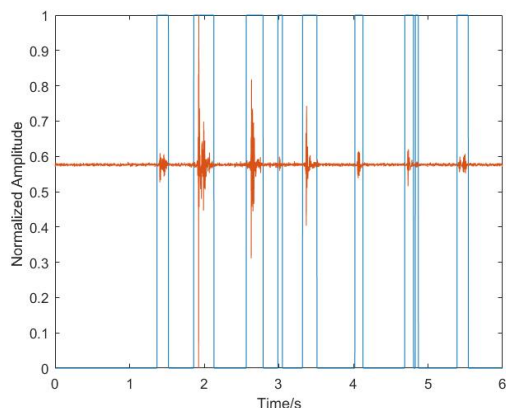


FIGURE 7. Normalized field data and event picking outputs.

The SNR for the three events is about 25dB, 10dB and -1dB. Fig.5(a) shows the STA/LTA feature for the noisy signals. The STA/LTA feature of the third event is not obvious so STA/LTA method can't handle with -1 dB data. It also reflects that the STA/LTA feature of weak signals is not obvious. There is another shortcoming of the STA/LTA method. If we chose a lower threshold for the start point, noise might be recognized as events. To avoid false alarm, the threshold can't be very small so the STA/LTA based outputs can't recognize the weak signal drawn in noise as shown in Fig.5(b). In comparison, we obtained GF using the same datasets and the results of

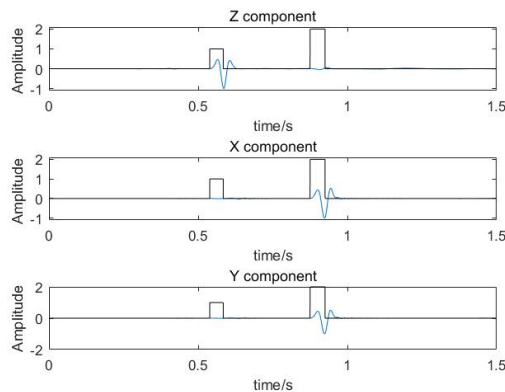


FIGURE 8. 3-Component datasets with labels.

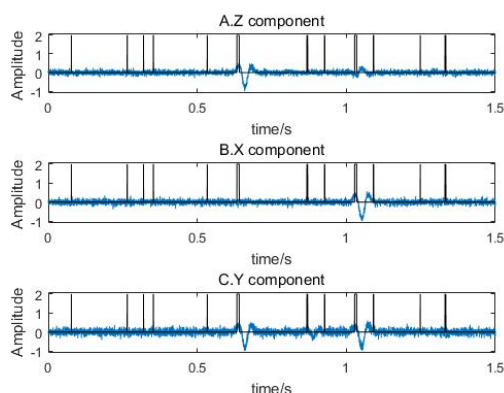


FIGURE 9. Output of the network without feature extraction for 3-C data.

the proposed method are shown in Fig.6(b). The results show that the proposed method has higher accuracy and anti-noise ability to pick microseismic events from noise. To evaluate the event picking performances of the proposed method, statistical analysis is applied to the test datasets. The result shows the error of the classification is only 0.054, which means the accuracy is 94.6%.

Then we apply the model to field datasets for picking human footsteps. The experiment aims to verify the model trained by synthetic datasets also can be applied to the real recorded data. The results are shown in Fig.7. The period of each event caused by human footstep is picked out even intensities of some events are very small, the picking results are accurate.

B. THREE-COMPONENT SYNTHETIC DATASET MODEL TO PICKING P- AND S-PHASES

Synthetic datasets were used to build and train a network with 3-component datasets. The synthetic datasets contain 600 3-C recordings and there are 6000 samples in each trace. To train the model, white noise of different intensities was added into the raw data. The average SNR is -5dB to 5dB. The datasets were divided into two parts: 60% of all are training datasets and the rest are the testing datasets.

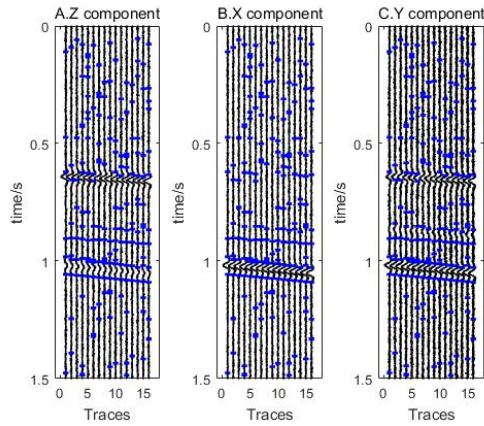


FIGURE 10. Phase picking results of each component (x,y and z). Blue solid lines are predicted onsets of S events and it's obvious that the network failed to detect P events. The accuracy of phase picking is quite poor and lots of wrong picks are in the traces.

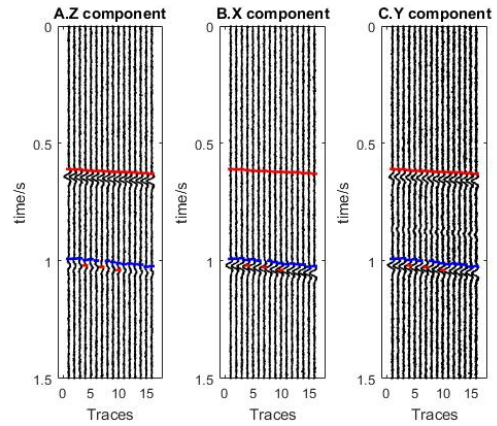


FIGURE 12. Output of the proposed network for all traces.

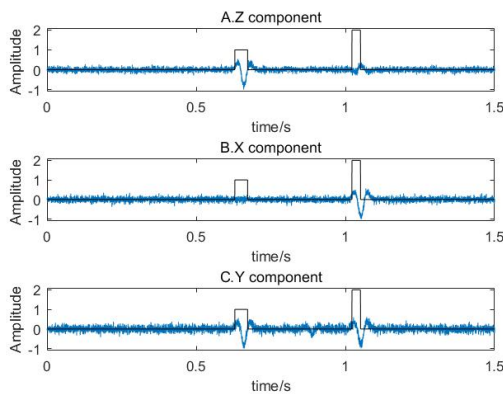


FIGURE 11. Output of the proposed network for a 3-C data.

We labeled recordings as “1” only for the first half cycle of P- event and “2” for the first half cycle of S- event shown in Fig.8. Labels for noise, P-phase and S-phase are actually (1, 0, 0), (0, 1, 0) and (0, 0, 1) for program realization.

The network was trained with/without GF to verify the effect of feature extraction. In order to prove that the extracted features can help reduce the size of the training datasets, first we fed three-component datasets into the network directly. The seismograms of each trace were divided into data frames, each frame has 200 sample points and the step for frameshift is 50-sample-point length. There are 4 layers in the network and lengths of the input layer, two hidden layers and a classification layer are 600 (200 for each frame, 3 components), 20, 10 and 3. The lengths of two hidden layers are 20 and 10. The length of the output layer is 3 because there are 3 classifications (noise, P-phase and S-phase).The activation function of each layer is the sigmoid function. Phase picking results (shown in Fig.9 and Fig.10) illustrated that the neural network can't pick the microseismic phases accurately. A lot of wrong predictions appear in traces and there is no need to discuss the accuracy of phase identification because not even a single P-event was predicted by the neural network.

TABLE 1. Accuracy of phase picking of the proposed method.

SNR(dB)	Accuracy of Phase Picking (%)		
	P and S -phase	P -phase	S -phase
-5	0.9477	0.9626	0.9614
0	0.9569	0.9677	0.9681
2.5	0.9613	0.9704	0.9715
5	0.9653	0.9734	0.9748
10	0.9702	0.9771	0.9782

Next, with the same training and testing datasets, a four-layer neural network with feature extraction is also designed. The training datasets were divided into data frames in the same way as mentioned above. Then the data frames were transformed into the GF matrix by a 64-Gammatone filter bank so the length of a GF is 64. We remained the outputs of the first 16 filters so the length of GF turns to 48 (16 for each component, 3 components). The numbers of neural units in each layer are 48, 20, 10 and 3. The testing datasets were transformed into the GF matrix and inputted into the trained neural network. The phase picking results (shown in Fig.11) of a single trace illustrate that the proposed method can recognize the phase of microseismic events even when the datasets are contaminated by noise.

The accuracy of phase picking is shown in Table 1. The results showed that the proposed method can pick phases accurately even when the raw data is added with -5 dB noise. Accurate phase picking verifies that the method is also robust. To pick the onsets of the phases, we can apply a simple post processor to obtain the arrival times of P- and S-phases. In Fig.11 there are ‘time windows’ for phase picking results, we regard the first starting point of time window as the onsets of the microseismic event phases.

We tested the phase-pickers with synthetic data as testing datasets. Red solid lines are picking results for P phases and blue solid lines are for S phases. The results are shown in Fig.12. As we can see that the P- and S- phases can be picked, but some ‘false alarm’ phase picking also obtained. Some constraints can be considered when dealing with outputs of classifiers.

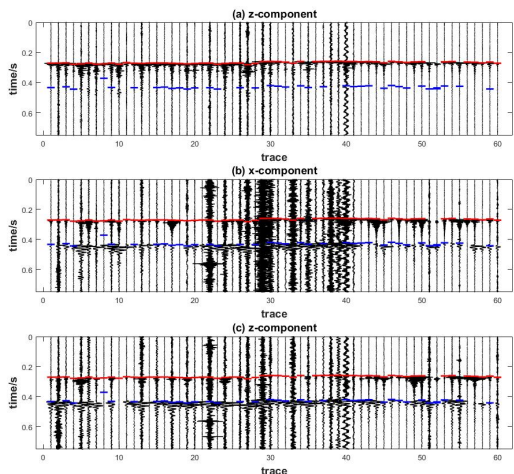


FIGURE 13. 3-C field data, the red solid lines are onsets of P events and blue solid lines are onsets of S events.

Comparing the phase picking results of two models (with/without feature extraction), with the same size of training datasets, hidden layers, and classification layer in the neural network, the model with the extracted features can pick P and S phases well but the model without extracted feature failed. The two neural networks also have two hidden layers and one output layer. The lengths of hidden layers are 20 and 10 while the length of the output layer is 3. If we use the training datasets directly, the length of the input layer is 600 (200 for each data frame, 3 components). The number of neural units in the first hidden layer is far less than the number in the input layer and there is too much information compression which resulted in great loss of desired information. So it's not surprising that the network can't perform well. The process of data compression should not be drastic. The model without feature extraction might perform better with more a complex structure and more neural units in the neural network but the complex structure of the model needs extra training datasets and results in more computation time.

The model with the extracted features can pick phases accurately. The structures of hidden layers and output later are the same size as the network without feature extraction. The length of the input layer is 48 and there is no big gap of numbers of neural units between the input layer and hidden layers. Most of the features from desired signals can be obtained and the network with feature extraction can perform well. The compared results suggest that the model with the extracted feature can be trained well with less size of datasets. So we can verify that the strategy with feature extraction can reduce the demand for large training datasets and labeling work furthermore the proposed method is of high accuracy to pick P and S phases of microseismic events.

C. THREE-COMPONENT FIELD DATA TEST

As mentioned above, the neural network was trained by synthetic datasets. Now we apply the model to field data sets, the datasets are from 60 3-C geophones (shown in Fig.13).

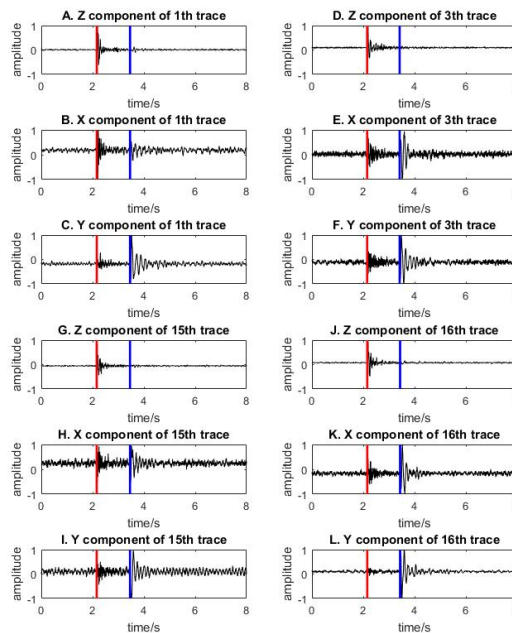


FIGURE 14. Phase picking results of each component (x,y and z) on the four traces of datasets shown in Fig.13. The red solid lines are onsets of P events and blue solid lines are onsets of S events.

The microseismic events were caused by hydraulic fracturing and the surface monitoring area is in Anda City, Heilongjiang Province of China. The datasets are contaminated by noise and the SNR of some traces are not very high. We use these field datasets (Fig.13) to test the performance of the proposed method. The neural network was trained by the same 3-component synthetic datasets mentioned above and we also add an output processor for picking phases. Red solid lines are noted for P-phases and blue solid lines are for S-phases. Results shown in Fig.13 illustrate that the proposed method can almost pick different phases (P or S) accurately although a few false phase picking indeed happens. In Fig.13, the proposed method picked almost all the P phases in the seismogram which means that the proposed method picks P events well in testing datasets. There are about 10 false pickings for S events but the results for picking S-events are still satisfying in the rest traces. We inferred that obvious coda (e.g. trace No.2 and 5) or relatively bad quality of datasets (eg. trace No.29) lead to false picking of S events. Details of phase picking results in 4 traces (trace No. 1, 3, 15 and 16) are shown in Fig.14. The proposed method picked all the phases at their onsets even the SNR of the signals are low (e.g. Fig.14 (E, F, H and I)). It's tough to pick phases manually by our naked eyes but the proposed method can pick and identify the phases. Although some false phase picking appears when dealing with S events, the proposed method to a certain degree can pick and identify phases automatically and accurately.

IV. CONCLUSION

We proposed a novel method using feature extraction and neural network to realize automatic phase picking. After

training the network with the synthetic datasets, both synthetic datasets and field datasets were used to test the network for phase picking. Experimental analyses verified that the network with feature extraction can be trained by relatively small size synthetic datasets so the calculation demand for training the model is decreased. Through designing different label strategies, the method realizes different phase picking effects according to different demands. Two cases were shown in this paper. For one component datasets the proposed method can pick out the whole period of microseismic events and the results can be applied to footstep detection; for three-component datasets the method can pick P- and S-phases of microseismic events and these phase picking results can be applied to fracture monitoring tasks. The experimental analyses showed that the proposed method is accurate and satisfying. However, we also noted that there were still a few false-alarm when the method dealt with three component field datasets. Some constraints can be added after the classifiers to decrease the 'false alarm'. In the following research, we will try to build a more complex model (more layers and neural units) with more efficient training strategies (constrains to the extracted features) to improve the accuracy of phase picking.

ACKNOWLEDGMENT

Thanks are extended to Prof. Ruizhao Yang for providing the field data and the suggestion for improving data redundancy.

REFERENCES

- [1] J. Akram, "Automatic p-wave arrival time picking method for seismic and micro-seismic data," in *Proc. CSPG CSEG CWLS Conv.*, 2011, pp. 1–4.
- [2] R. V. Allen, "Automatic earthquake recognition and timing from single traces," *Bull. Seismol. Soc. Amer.*, vol. 68, no. 5, pp. 1521–1532, 1978.
- [3] M. Lee, J. Byun, D. Kim, J. Choi, and M. Kim, "Improved modified energy ratio method using a multi-window approach for accurate arrival picking," *J. Appl. Geophys.*, vol. 139, pp. 117–130, Apr. 2017.
- [4] A. Kwietniak, "Detection of the long period long duration (LPLD) events in time-and frequency-domain," *Acta Geophys.*, vol. 63, no. 1, pp. 201–213, Feb. 2015.
- [5] R. Zhang and L. Zhang, "Method for identifying micro-seismic P-arrival by time-frequency analysis using intrinsic time-scale decomposition," *Acta Geophys.*, vol. 63, no. 2, pp. 468–485, Apr. 2015.
- [6] T. Wang, M. Zhang, Q. Yu, and H. Zhang, "Comparing the applications of EMD and EEMD on time-frequency analysis of seismic signal," *J. Appl. Geophys.*, vol. 83, pp. 29–34, Aug. 2012.
- [7] N. Hargreaves, R. Wombell, and R. Ver West, "Multiple attenuation using an apex-shifted radon transform," in *Proc. 65th EAGE Conf. Exhib.*, Jun. 2003, pp. 1929–1932.
- [8] J. I. Sabbione, M. D. Sacchi, and D. R. Velis, "Radon transform-based microseismic event detection and signal-to-noise ratio enhancement," *J. Appl. Geophys.*, vol. 113, pp. 51–63, Feb. 2015.
- [9] J. Zheng, J.-R. Lu, T.-Q. Jiang, and Z. Liang, "Microseismic event denoising via adaptive directional vector median filters," *Acta Geophys.*, vol. 65, no. 1, pp. 47–54, Mar. 2017.
- [10] R. Hu and Y. Wang, "A first arrival detection method for low SNR micro-seismic signal," *Acta Geophys.*, vol. 66, no. 5, pp. 945–957, Oct. 2018.
- [11] J. I. Sabbione and D. R. Velis, "A robust method for microseismic event detection based on automatic phase pickers," *J. Appl. Geophys.*, vol. 99, pp. 42–50, Dec. 2013.
- [12] G. E. Hinton, "Reducing the dimensionality of data with neural networks," *Science*, vol. 313, no. 5786, pp. 504–507, Jul. 2006.
- [13] D. Maity and I. Salehi, "Neuro-evolutionary event detection technique for downhole microseismic surveys," *Comput. Geosci.*, vol. 86, pp. 23–33, Jan. 2016.
- [14] Z. E. Ross, M. Meier, E. Hauksson, and T. H. Heaton, "Generalized seismic phase detection with deep learning," *Bull. Seismol. Soc. Amer.*, vol. 108, no. 5A, pp. 2894–2901, Oct. 2018.
- [15] T. Perol, M. Gharbi, and M. Denolle, "Convolutional neural network for Earth quake detection and location," *Sci. Adv.*, vol. 4, no. 2, Feb. 2018, Art. no. e1700578.
- [16] W. Zhu and G. C. Beroza, "PhaseNet: A deep-neural-network-based seismic arrival time picking method," *Geophys. J. Int.*, pp. 261–273, Oct. 2018.
- [17] J. Zheng, J. Lu, S. Peng, and T. Jiang, "An automatic microseismic or acoustic emission arrival identification scheme with deep recurrent neural networks," *Geophys. J. Int.*, vol. 212, no. 2, pp. 1389–1397, Feb. 2018.
- [18] D. Maity, F. Aminzadeh, and M. Karrenbach, "Novel hybrid artificial neural network based autopicking workflow for passive seismic data," *Geophys. Prospecting*, vol. 62, no. 4, pp. 834–847, Jul. 2014.
- [19] K. Kaur, M. Wadhwa, and E. K. Park, "Detection and identification of seismic P-Waves using artificial neural networks," in *Proc. Int. Joint Conf. Neural Netw. (IJCNN)*, Aug. 2013, pp. 1–6.
- [20] R. F. Lyon, "Cascades of two-pole-two-zero asymmetric resonators are good models of peripheral auditory function," *J. Acoust. Soc. Amer.*, vol. 130, no. 6, pp. 3893–3904, Dec. 2011.
- [21] X. Zhao and D. Wang, "Analyzing noise robustness of MFCC and GFCC features in speaker identification," in *Proc. IEEE Int. Conf. Acoust., Speech Signal Process.*, May 2013, pp. 7204–7208.
- [22] B. R. Glasberg and B. C. J. Moore, "Derivation of auditory filter shapes from notched-noise data," *Hearing Res.*, vol. 47, nos. 1–2, pp. 103–138, Aug. 1990.
- [23] M. Slaney, "An efficient implementation of the Patterson Holdsworth auditory filter bank," 1993.
- [24] R. D. Patterson, J. Holdsworth, and M. Allerhand, "Auditory models as preprocessors for speech recognition," in *The Auditory Process. Speech: From Auditory Periphery to Words*. Berlin, Germany: Mouton de Gruyter, 1992, pp. 67–89.
- [25] G. E. Hinton, S. Osindero, and Y.-W. Teh, "A fast learning algorithm for deep belief nets," *Neural Comput.*, vol. 18, no. 7, pp. 1527–1554, Jul. 2006.



TIANQI JIANG received the B.S. degree in geophysics from the China University of Mining and Technology at Beijing, Beijing, China, in 2014, where he is currently pursuing the Ph.D. degree with the College of Geoscience and Surveying Engineering. His research interest includes applied machine learning methods in microseismic data process.



JING ZHENG received the B.S. degree in electronic science and technology and the Ph.D. degree in communication and information system from Beihang University, Beijing, China, in 2006 and 2011, respectively. From 2011 to 2015, she was a Lecturer with the College of Geoscience and Surveying Engineering, China University of Mining and Technology at Beijing, Beijing, where she has been an Assistant Professor, since 2015. Her research interests include the development of GPR and seismic data processing techniques using machine learning methods.

...